

Figure S1 Aftershocks space-time evolution in four periods. (a) $M_L \geq 2$ aftershocks distribution from August 24th, to October 25th, 2016; (b) $M_L \geq 2$ aftershocks distribution from October 26th, to October 29th, 2016; (c) $M_L \geq 2$ aftershocks distribution from October 30th, 2016 to January 17th, 2017; (d) $M_L \geq 2$ aftershocks distribution from January 18th, to June 30th, 2017. The red star corresponds to the epicenter of August 24th, 2016 earthquake, the green star denotes the epicenter of October 26th, 2016 earthquake, the blue star denotes the epicenter of October 30th, 2016 earthquake and the golden yellow star denotes the epicenter of January 18th, 2017 earthquake [1].

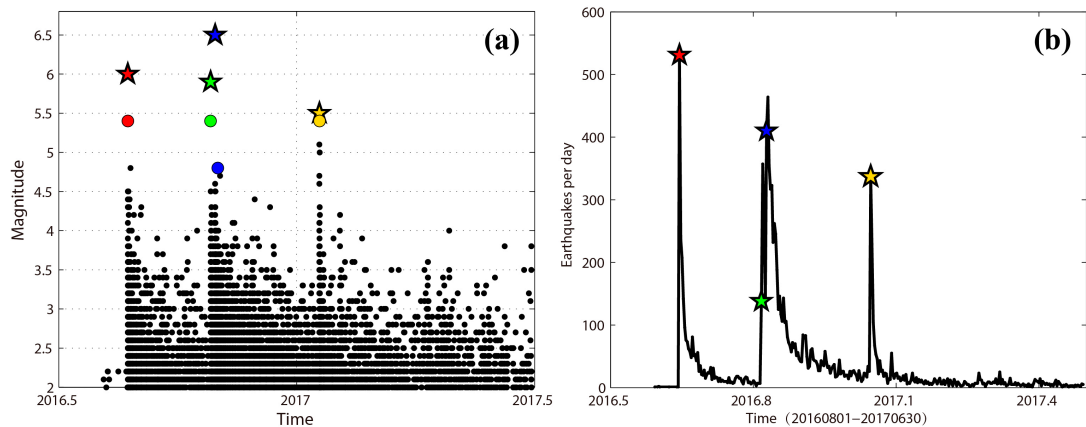


Figure S2 (a) Earthquake magnitude versus time (from August 1st, 2016 to June 30th, 2017, $M \geq 2$); stars denotes the three main event and circles indicate the largest aftershock of every event (Here we should note that the earthquake represented by green circle occurred before the Event B); (b) seismicity rate ($M \geq 2$) in the area

immediately surrounding the 2016 Italian earthquake sequence (from August 1st, 2016 to June 30th, 2017). The red star corresponds to the epicenter of August 24th, 2016 earthquake, the green star denotes the epicenter of October 26th, 2016 earthquake, the blue star denotes the epicenter of October 30th, 2016 earthquake and the golden yellow star denotes the epicenter of January 18th, 2017 earthquake [1].

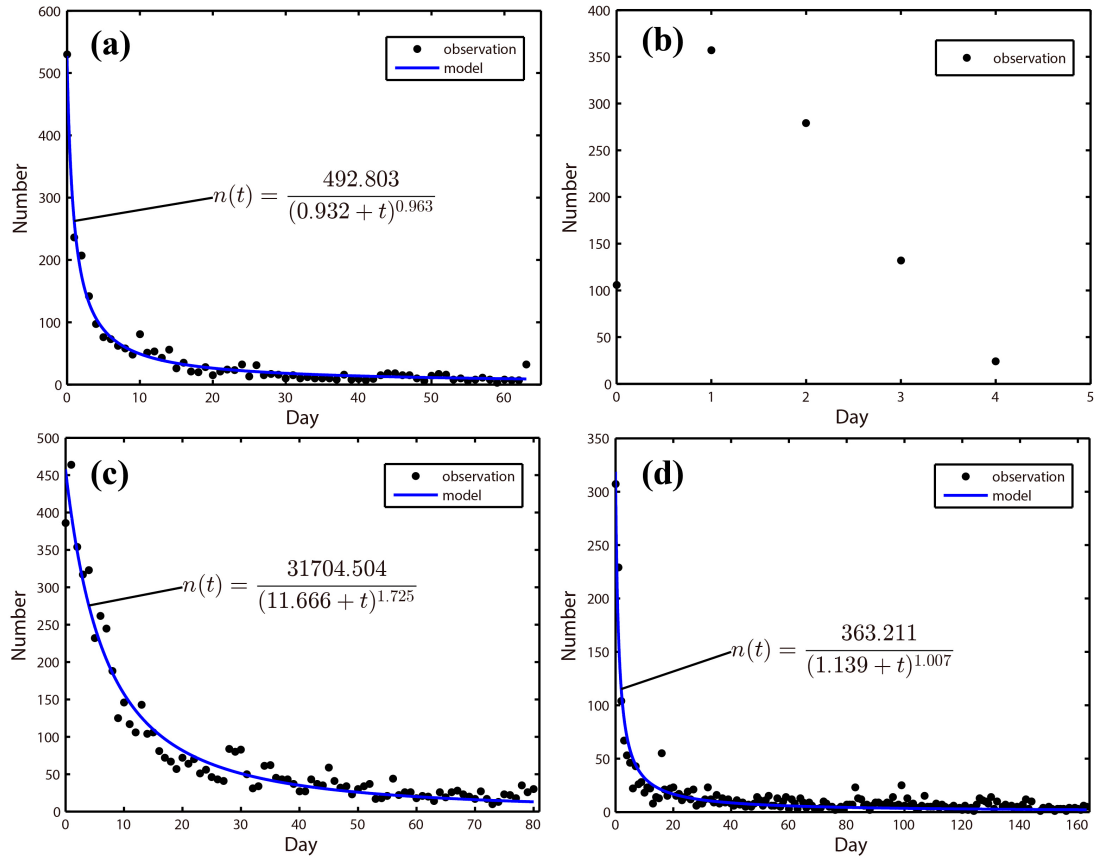


Figure S3 The decay histories of the first seismic subsequences and fitting result (blue curves with the modified Omori's law); (a) from August 24th, to October 25th, 2016; (b) from October 26th, 2016 to October 29th, 2016 (just decay history); (c) from October 30th, 2016 to January 17th, 2017; (d) from January 18th, to June 30th, 2017.

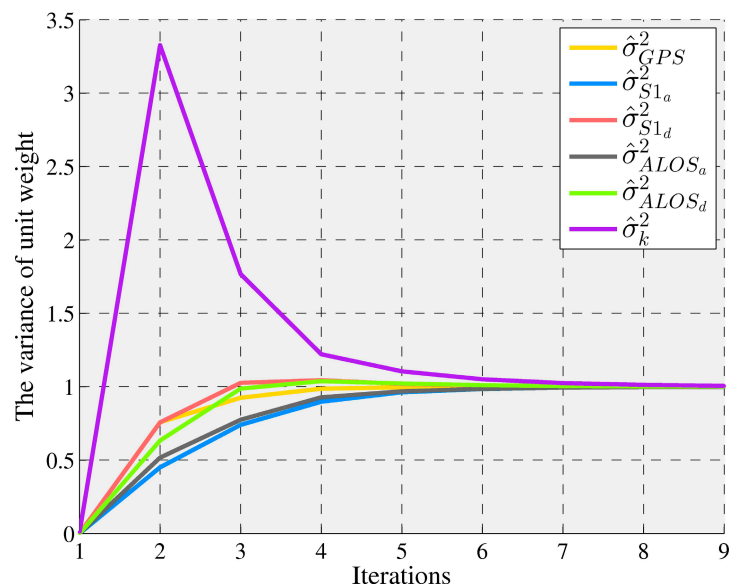


Figure S4. Estimates of the variance of unit weight over different iterations steps in the inversion procedure of 2016 Amatrice earthquake.

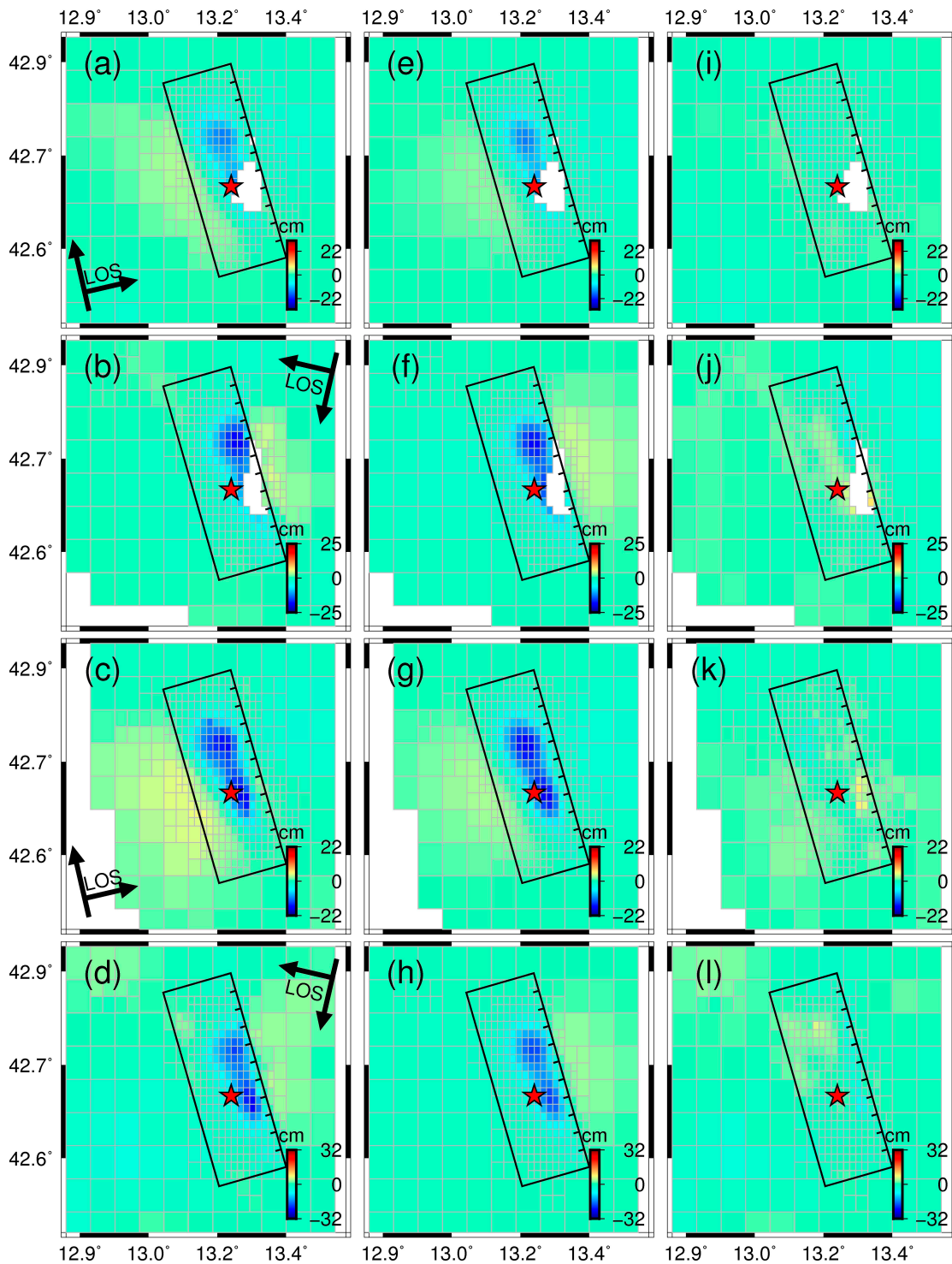


Figure S5. Comparison of observed and modeled LOS displacements from SAR observations. (a-d) Observations, (e-h) model predictions, and (i-l) residuals. (a, e, i) corresponding to the ascending Sentinel-1 track T117; (b, f, j) corresponding to the descending Sentinel-1 track T022; (c, g, k) corresponding to the ascending ALOS-2 track P197A; (d, h, l) corresponding to the descending ALOS-2 track P092D. The red star corresponds to the epicenter of August 24th, 2016 Amatrice earthquake [1]. The black rectangle indicates the surface projection of the estimated

fault plane.

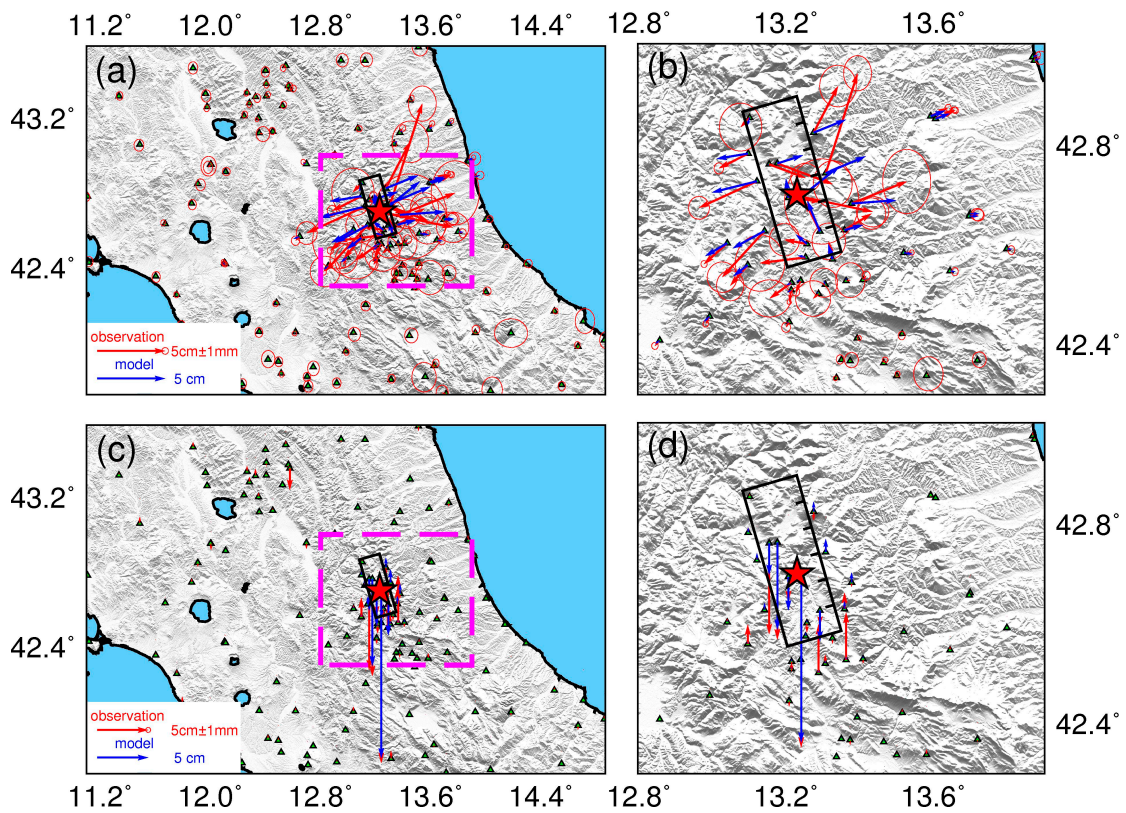


Figure S6 Observed (red) and modeled (blue) horizontal coseismic displacement of August 24th, 2016 Amatrice earthquake (a). The pink rectangle outlines the area in subplot (b). Observed (red) and modeled (blue) vertical coseismic displacement of August 24th, 2016 Amatrice earthquake (c). The pink rectangle outlines the area in subplot (d). Ellipses on the horizontal component depict the 95% confidence level of formal uncertainties. The red star corresponds to the epicenter of August 24th, 2016 Amatrice earthquake [1]. The black rectangle indicates the surface projection of the estimated fault plane.

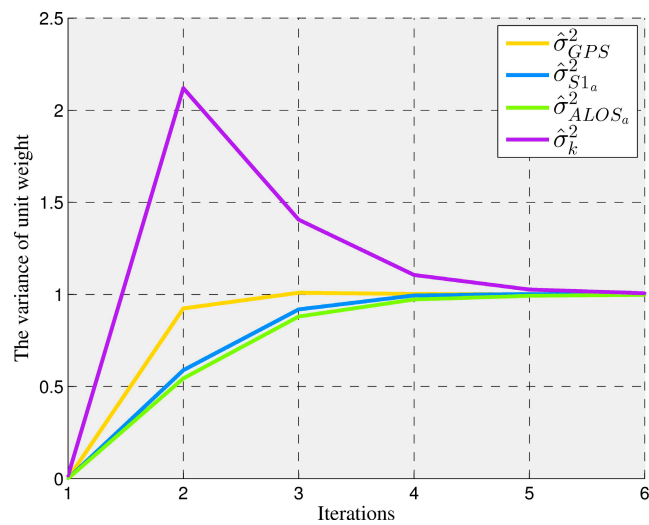


Figure S7. Estimates of the variance of unit weight over different iterations steps in the inversion procedure

of 2016 Visso earthquake.

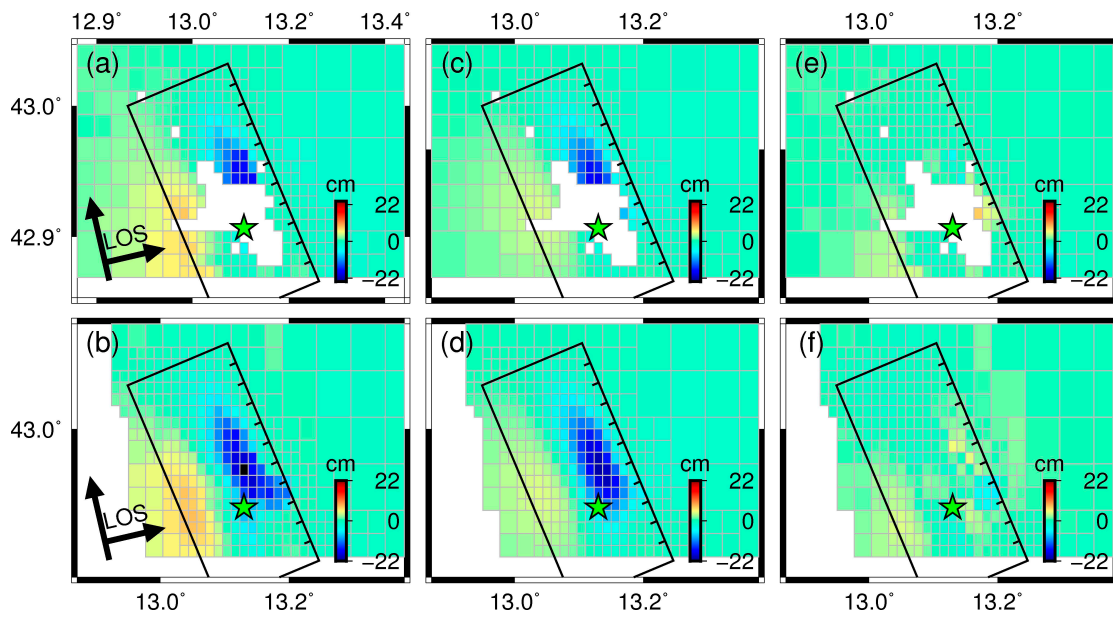


Figure S8. Comparison of observed and modeled LOS displacements from SAR observations. (a-b) Observations, (c-d) model predictions, and (e-f) residuals. (a, c, e) corresponding to the ascending Sentinel-1 track T044; (b, d, f) corresponding to the ascending ALOS-2 track P197. The green star corresponds to the epicenter of October 26th, 2016 Visso earthquake [1]. The black rectangle indicates the surface projection of the estimated fault plane.

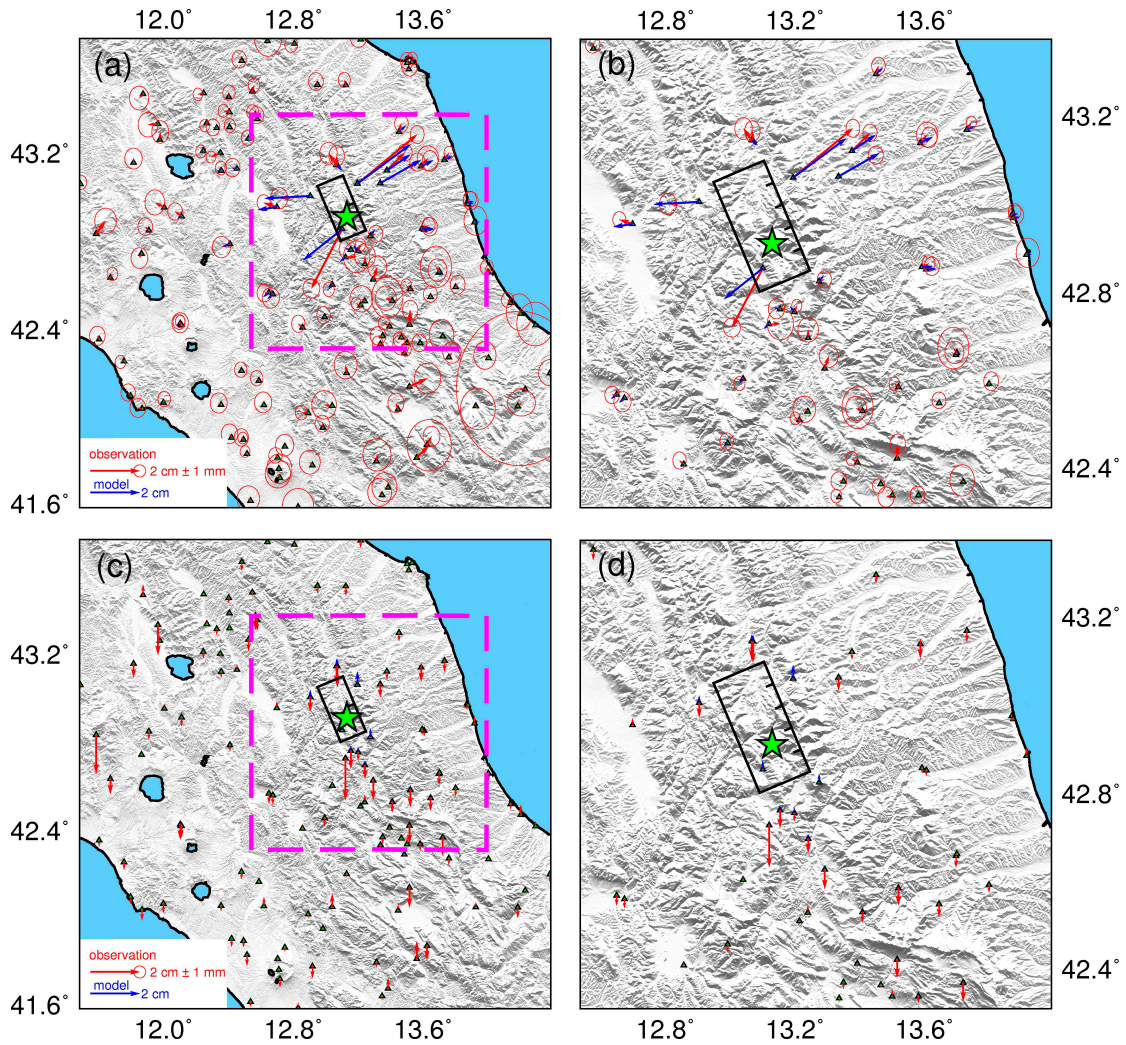


Figure S9 Observed (red) and modeled (blue) horizontal coseismic displacement of October 26th, 2016 Visso earthquake (a). The pink rectangle outlines the area in subplot (b). Observed (red) and modeled (blue) vertical coseismic displacement of October 26th, 2016 Visso earthquake(c). The pink rectangle outlines the area in subplot (d). Ellipses on the horizontal component depict the 95% confidence level of formal uncertainties. The green star corresponds to the epicenter of October 26th, 2016 Visso earthquake [1]. The black rectangle indicates the surface projection of the estimated fault plane.

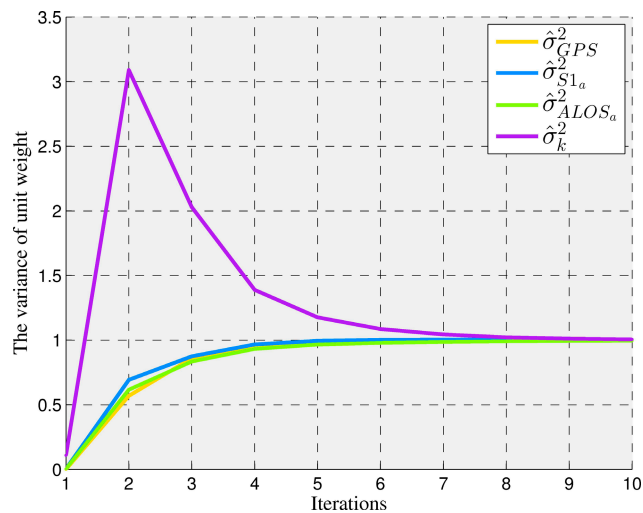


Figure S10. Estimates of the variance of unit weight over different iterations steps in the inversion procedure of 2016 Norcia earthquake.

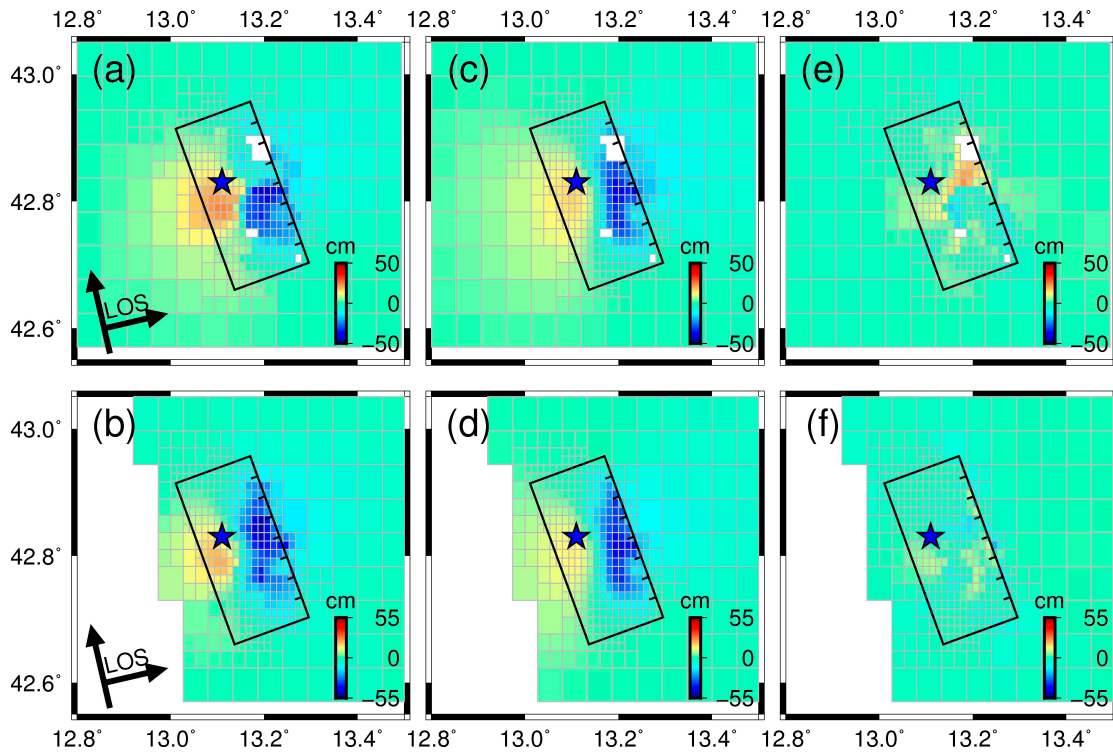


Figure S11. Comparison of observed and modeled LOS displacements from SAR observations. (a-b) Observations, (c-d) model predictions, and (e-f) residuals. (a, c, e) corresponding to the ascending Sentinel-1 track T044; (b, d, f) corresponding to the ascending ALOS-2 track P196. The blue star corresponds to the epicenter of October 30th, 2016 Norcia earthquake [1]. The black rectangle indicates the surface projection of the estimated fault plane.

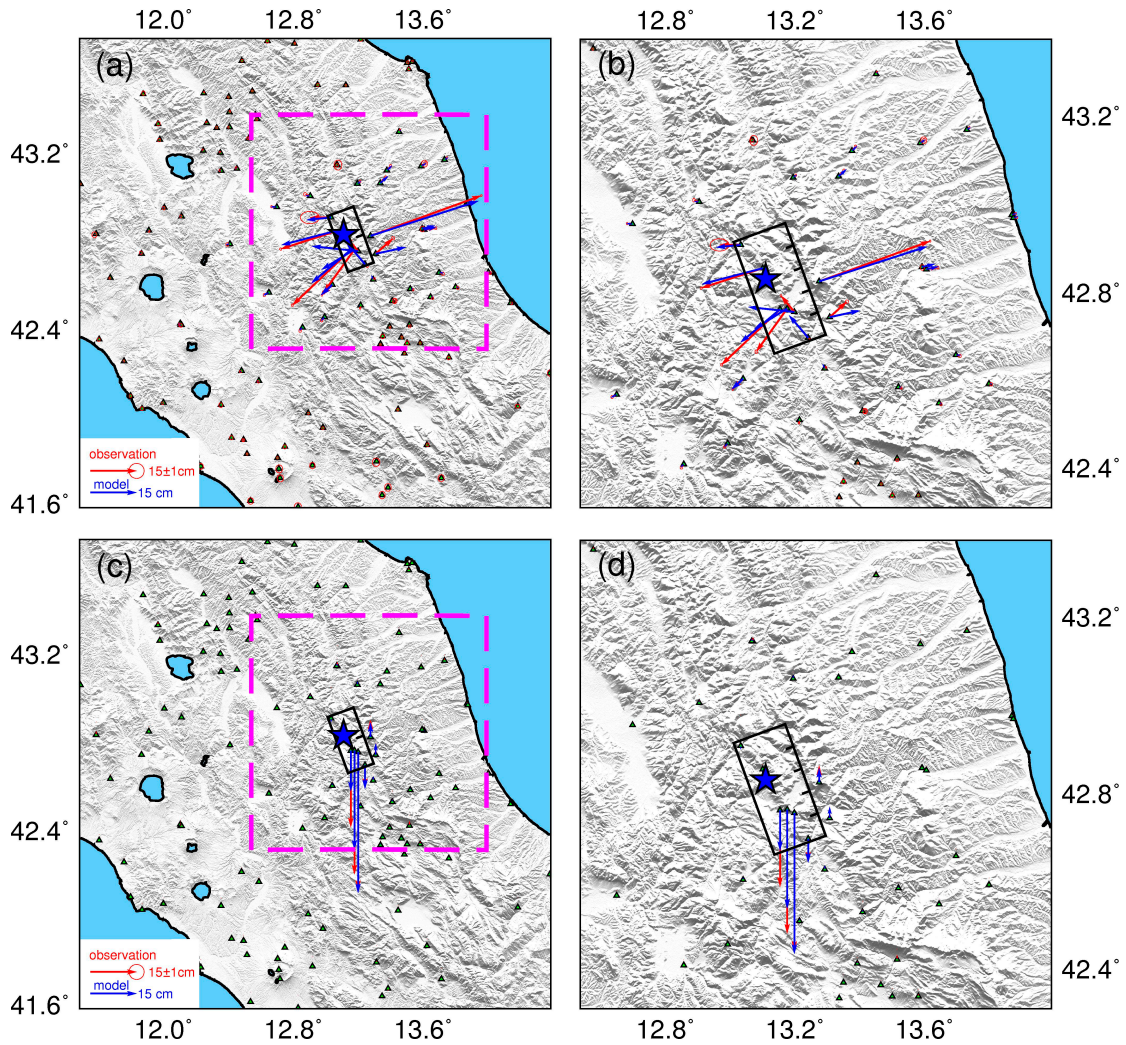


Figure S12 Observed (red) and modeled (blue) horizontal coseismic displacement of October 30th, 2016 Norcia earthquake (a). The pink rectangle outlines the area in subplot (b). Observed (red) and modeled (blue) vertical coseismic displacement of October 30th, 2016 Norcia earthquake (c). The pink rectangle outlines the area in subplot (d). Ellipses on the horizontal component depict the 95% confidence level of formal uncertainties. The blue star corresponds to the epicenter of October 30th, 2016 Norcia earthquake [1]. The black rectangle indicates the surface projection of the estimated fault plane.

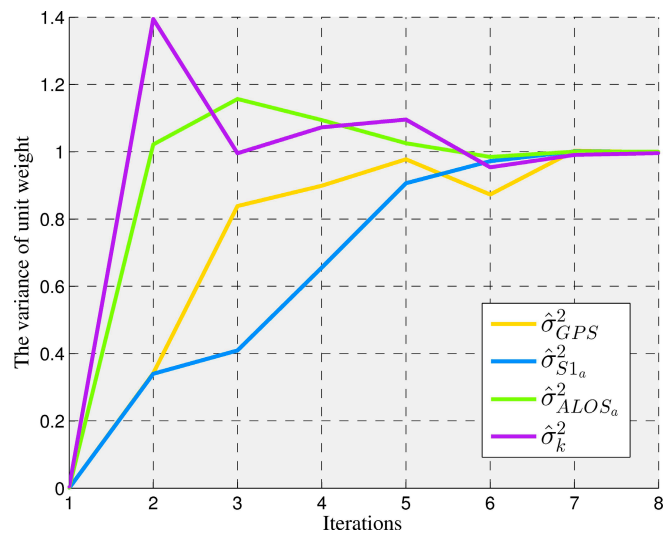


Figure S13. Estimates of the variance of unit weight over different iterations steps in the inversion procedure of 2017 Campotosto earthquake.

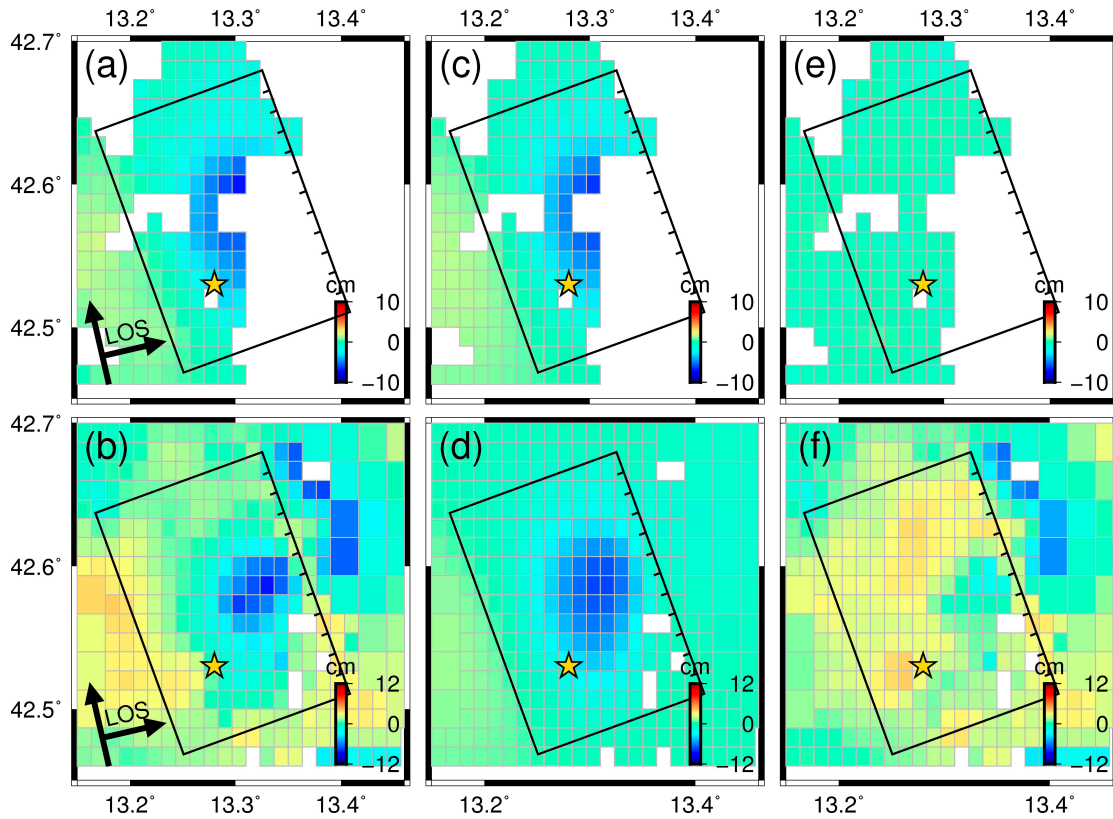


Figure S14. Comparison of observed and modeled LOS displacements from SAR observations. (a-b) Observations, (c-d) model predictions, and (e-f) residuals. (a, c, e) corresponding to the ascending Sentinel-1 track T117; (b, d, f) corresponding to the ascending ALOS-2 track P197. The golden yellow star corresponds to the epicenter of January 18th, 2017 Campotosto earthquake [1]. The black rectangle indicates the surface projection of the estimated fault plane.

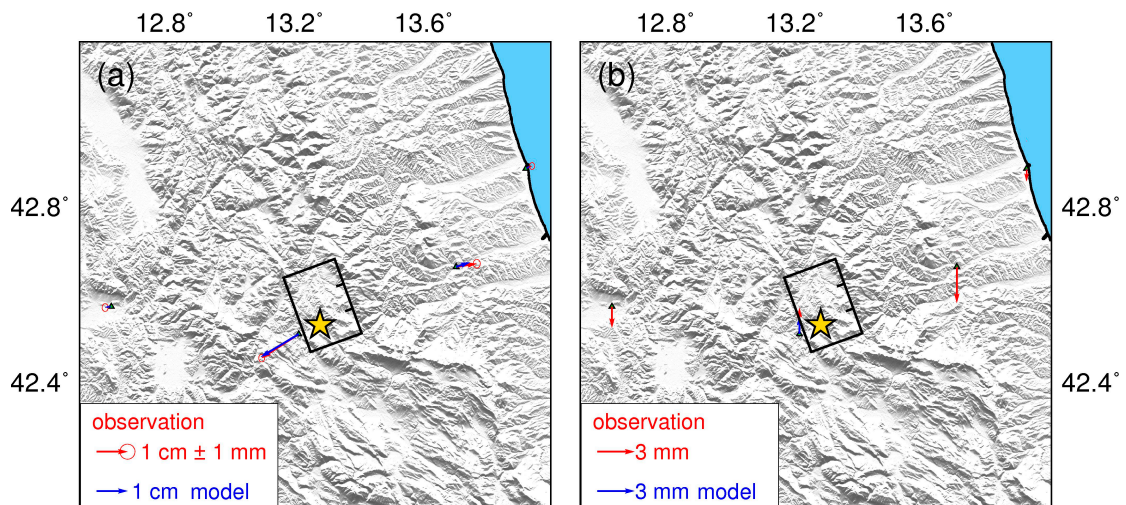


Figure S15 Observed (red) and modeled (blue) horizontal coseismic displacement of January 18th, 2017 earthquake (a). Observed (blue) and modeled (red) vertical coseismic displacement of January 18th, 2017 earthquake (b).

Ellipses on the horizontal component depict the 95% confidence level of formal uncertainties. The golden yellow star corresponds to the epicenter of January 18th, 2017 Campotosto earthquake [1]. The black rectangle indicates the surface projection of the estimated fault plane.

Table S1 Input parameters used in the calculation of Static Coulomb Stress Change on the fault of the 2016 Visso earthquake

Poisson	0.25
Shear modulus	$3.3 \times 10^{10} \text{ N/m}^2$
Friction coefficient	0.4
source fault	the fault of the 2016 Amatrice earthquake
receiver fault	the fault of the 2016 Visso earthquake

References

1. Institute of Geophysics and Volcanology. Available online: <http://info.terremoti.ingv.it/> (accessed on 30 June, 2017).